Sialoglycans modulate Siglec-5 – TLR4 Interactions in Osteoarthritis

Authors: Loise Råberg[1], Fan Jia[1], Ula von Mentzer[1], Niclas G. Karlsson[2], Alexandra Stubelius[1*]

Affiliations:
[1] Division of Chemical Biology, Department of Life Sciences, Chalmers University of Technology, Gothenburg, SE-412 96, Sweden.
[2] Department of Life Sciences and Health, Faculty of Health Sciences, Oslo Metropolitan University Oslo Metropolitan University, Oslo, Norway
[*]**Corresponding author:**
Alexandra Stubelius (alexandra.stubelius@chalmers.se)
Chalmers University of Technology
Department of Life Sciences
Division of Chemical Biology
Kemigården 4
SE-412 96 Göteborg,
Sweden
+46(0)31-772 4101
Conflict of interest: NK authored a patent involving OA diagnostics, and NK hold equity in Lynxon AB. The other authors have declared that no conflict of interest exists.
Keywords: Osteoarthritis, Monocytes, Siglec-5, Sialic Acid, TLR4

Summary:
Osteoarthritis (OA) is characterized by chronic, low-grade inflammation that contributes to cartilage degradation and joint pain. We previously identified Siglecs in the synovial fluid of OA patients (OA-SF), and together with studies implicating Siglecs in arthritic diseases prompted us to investigate the interplay between Siglec-5, Siglec-9, and TLR4 in monocyte regulation during OA. Flow cytometric profiling revealed an inverse correlation between Siglec-5 expression and TLR4 activity, but not Siglec-9, suggesting that Siglec-5 engagement may suppress inflammatory responses.
To gain mechanistic insights, we compared monocytes stimulated with OA-SF to those treated with key inflammatory mediators –M-CSF, LPS, and sialidase – to assess patient-specific inflammatory pathways and phenotypes. Further analysis of the TLR4-Siglec crosstalk using the small molecule inhibitor TAK-242 confirmed that sialoglycans modulate TLR4-driven inflammation. Notably, OA-SF from patients with high-grade inflammation led to monocyte expression profiles similar to LPS- or sialidase treated cells, reinforcing the role of sialylation in regulating inflammatory severity in OA. These findings reveal a TLR4-Siglec-5 axis modulated by sialylation, highlighting a potential strategy for mitigating inflammation and preserve joint integrity in OA.

INTRODUCTION

Osteoarthritis (OA) is the most common degenerative joint disorder worldwide, characterized by synovitis, cartilage degradation and subchondral bone remodeling that severely impacts quality of life [1]. This complex condition involving mechanical stress and inflammatory pathways displays significant variability between patients. Persistent inflammation stem from both tissue-resident and infiltrating immune cells, including monocytes, which play key roles in perpetuating inflammation [2,3]. Upon recruitment, monocytes are polarized into a pro-inflammatory phenotype in response to the local environment, contributing to the cycle of tissue damage and degeneration of cartilage [4,5]. The multifactorial nature of OA coupled to the limited regenerative capacity of cartilage, has posed a major challenge for developing effective treatments. Despite extensive efforts, clinical trials targeting cytokines such as IL1B and TNFa have not yielded significant therapeutic benefits, underscoring the need for alternative mechanistic insights and novel intervention strategies.

Recent advances in nanotherapeutics has offered promising new approaches, as they can deliver drugs to the deeply embedded cells in the cartilage responsible for OA development. In our previous work, we explored the interactions between a family of small dendritic polyamidoamine (PAMAM)-based NPs and synovial fluid (SF) proteins from OA patients [6]. Notably, we identified a high abundance of Sialic acid-binding immunoglobulin-like lectin-5 (Siglec-5) in the protein corona, suggesting a potential role in OA pathogenesis.
Siglecs are gaining increasing attention in several diseases, including cancer, sepsis, and autoimmune disorders due to their immunomodulatory functions and potential for therapeutic targeting [7]. Siglec-9 has been found in sepsis and arthritis, and Siglec-15 plays an important role in macrophage fusion into osteoclasts [8 9,10]. Through their affinity to sialic acid (Sia), Siglecs act as key regulators of monocyte activation to counterbalance pro-inflammatory pathways. Siglec-5 is mostly found on cell surfaces on monocytes, macrophages, and T cells, soluble Siglec-5 was shown to inhibit $CD8^+$ T cell proliferation in sepsis, and soluble Siglec-9 demonstrated immunosuppressive effects on macrophages in arthritis models [8,11].
Interestingly, a study demonstrating that lipopolysaccharide (LPS) triggers sialidase activity, also found that Siglec-E, the mouse ortholog of human Siglec-9, counteracts this process by binding Sia residues on Toll-like receptor 4 (TLR4). This leads to TLR4 internalization and reduced inflammation. Siglec-5 and Siglec-9 have both shown high affinity to TLR4, indicating their immunomodulatory role [12]. However, Siglec-5 has not been as extensively studied as Siglec-9, which could be due to lack of a mouse ortholog [11,13].
Central to OA-associated inflammation is the activation of pattern recognition receptors, particularly TLR4, which recognizes structural fragments of damaged cartilage [14,15]. Solubilized fragments of glycoproteins such as collagen type-II, hyaluronan, aggrecan, and lubricin are present in OA synovial fluid (SF) can function as damage-associated molecular patterns (DAMPs), thereby exacerbating joint inflammation [16-18]. Through the NF-κB pathway pro-inflammatory cytokines such as IL-1, IL-6, IL-8, and tumor necrosis factor (TNFα) are released in the joint, aggravating joint degradation and OA symptoms [3,19-22].

TLR4 activity is influenced by its sialylation pattern and internalization dynamics. Studies have shown that Sia on monocyte surfaces, regulated by enzymes such as sialyltransferases and sialidases, plays a pivotal role in modulating TLR4 signaling [12,23,24]. It has been shown that LPS can trigger sialidase relocation to the cell surface, where it desialylates TLR4 and promotes its activation [25]. In general, endogenous sialyltransferases and sialidases activities are regulated upon monocyte activation and differentiation, and they have been shown to be involved in OA pathogenesis [26]. In addition, the levels of Sia on the surface of a cell have been directly linked to the cells' overall maturation and functional responsiveness [27,28].

As we had found Siglec-5 in the SF of OA patients, the purpose of this study was to investigate the interplay between Siglec-5, Siglec-9, and TLR4 in monocyte regulation during OA. Flow cytometric profiling revealed an inverse correlation between Siglec-5 expression and TLR4 activity, suggesting that engaging Siglec-5 dampens excessive inflammatory responses. To gain mechanistic understanding we employed ex vivo stimulations including macrophage-colony stimulating factor (M-CSF), IL1β/TNFα, LPS, and Sialidase to understand patient-specific inflammatory pathways and phenotypes. Further insights of crosstalk between TLR4 with Siglec-5 and siglec-9, was gained through inhibition of TLR4 signaling using the small molecule inhibitor TAK-242. Our findings suggest that Siglec-5 can serve as a modulator of TLR4-driven low-grade inflammation, as patients with high-grade inflammation showed similar profiles as LPS or Sialidase-treated cells, indicating that Sia is a critical regulator of high-grade OA inflammation. Overall, our findings suggest that Siglec-5, but not Siglec-9, through Sia expression on cells could offer a therapeutic strategy to mitigate inflammation, reduce cartilage degradation, and alleviate pain in OA patients.

RESULTS

Siglec-5 can be found in synovial fluid from osteoarthritis patients and negatively correlates with TLR4 expression on monocytes

NPs can be used as enrichment tools to identify rare but impactful proteins associated with OA pathogenesis. In a previous study, we developed a set of NPs which we incubated with SF and further analyzed through proteomics [6]. Amongst the 14 most abundant proteins found in association with the NP we identified Siglec-5 as one of the most abundant (Figure 1A). To explore signaling pathways involved with Siglec-5, we used the Interactome database and discovered a close relationship between Siglec-5 and TLR4 (Figure 1B), which both can be found on monocytes.

Monocytes and macrophages are the most abundant immune cells of the joint in OA [15]. Their different functions can be characterized into subsets based on their expression of CD14 and CD16. Classical monocytes with phagocytic capabilities express $CD14^{+}CD16^{-}$; intermediate monocytes express $CD14^{+}$, $CD16^{+}$ and perform antigen presentation and secrete cytokines, whereas non-classical express $CD14^{-}CD16^{+}$ and perform complement and Fc gamma-mediated phagocytosis [29,30]. The intermediate subset has been found in greater abundance in the joint of OA patients [15].

To investigate the capacity of OA-derived SF to regulate monocyte receptor expression, flow cytometric evaluation was performed based on CD14 and CD16 (gating strategy shown in Figure S1A-F). The overall fraction of isolated monocytes (85.9%) as well as relative fraction of monocyte subsets were determined (Figure S2A and S1B). The monocytes were then further subdivided into their expression of TLR4, Siglec-5, and Siglec-9. Monocytes were stimulated with SFs collected from seven OA patients scheduled for total knee joint replacement.

We investigated how OA-patient derived SFs stimulated the differentiation of monocyte populations with respect to their expression of CD16, TLR4, Siglec-5, and Siglec-9. We observed variations in both CD16 (Figure 1C) and TLR4 expression on the monocytes (Figure 1D). In contrast to the TLR4 levels, multiple patient-derived SFs lead to a significant upregulation in Siglec-5 expression on monocytes (Figure 1E). In contrast to previous murine studies, Siglec-9 was only upregulated in one patient (Figure 1F).

Correlation analysis confirmed an inverse relationship between Siglec-5 with TLR4 and intermediate monocytes (Figure 1G and 1H), whereas no correlation was observed between, Siglec-9 with TLR4 and intermediate monocytes (Figure 1I and 1J). Furthermore, a correlation between Siglec-5 to Siglec-9, and intermediate monocytes to TLR4 could not be established (Figure S3A and S3B).

All monocytes expressed Siglec-5 and Siglec-9 (not shown), whereas the percentage $TLR4^{+}$ monocytes were mainly found in the intermediate population (Figure 1K). All patient-derived SFs except one, generated an intermediate monocyte population consisting of > 50% out of the whole population, baseline levels (0hrs) were <10% (Figure S2B). Before OA-SF stimulation, monocytes displayed a baseline ratio between classical, intermediate, and non-classical monocytes [31]. Concurrent with this, the classical monocytes decreased compared to baseline levels and non-classical monocytes were not present anymore. At baseline, classical monocytes displayed the highest expression of TLR4, Siglec-5, and Siglec-9 (Figure M-O). In summary, the monocytes shifted toward the intermediate subset after SF stimulation. Correlation analysis revealed an inverse relationship between Siglec-5, TLR4, and intermediate monocytes, but not with Siglec-9, suggesting complex interactions in OA inflammation.

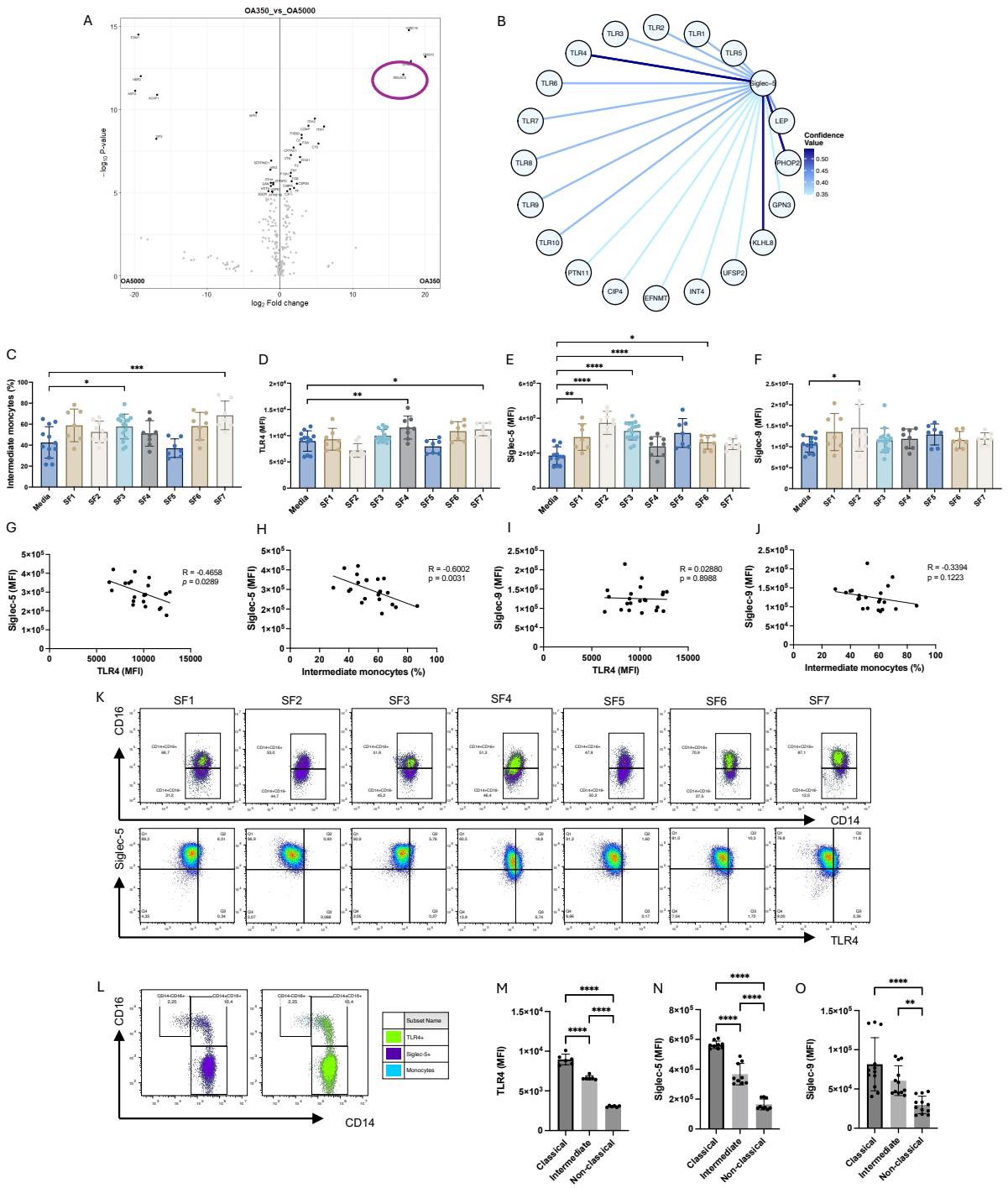

Figure 1. Siglec-5 can be found in synovial fluid from osteoarthritis patients and negatively correlates with TLR4 expression on monocytes

(A) Volcano plot displaying the proteins detected in the protein corona of $PAMAM_{5000}$ and $PAMAM_{350}$, here denoted OA5000 and OA350 using proteomics analysis. Siglec-5 is indicated with a circle.

(B) Protein-protein interaction network visualized from the IntAct database. Strong evidence of interaction appears to TLR4, PHOP2, and KLHL8, as evidenced by high confidence score. The illustration was adopted from the website and improved using R.

(C) Percentage intermediate monocytes ($CD14^+CD16^+$) after 24hrs in media control and SF1-7 (*n*=3 from three biological replicates).

(D-F) Median fluorescence intensity (MFI) of TLR4, Siglec-5, and Siglec-9 on the cell membrane (*n*=3 from three biological replicates).

(G-J) Correlation between Siglec-5 to TLR4 and intermediate monocytes, and between Siglec-9 to TLR4 and intermediate monocytes.

(K) Representative flow cytometric dot plots displaying the ratio between classical and intermediate monocytes, where blue represents both subsets, purple represents Siglec-5^+ cells, and green represents $TLR4^+$ cells.

(L) Baseline levels (0hrs) of classical, intermediate, and non-classical subsets, where blue color represents all monocytes, purple color represents Siglec-5^+, and green represents $TLR4^+$ cells.

(M-O)MFI of TLR4, Siglec-5, and Siglec-9 in monocyte subsets. Data is presented as mean percentage or MFI (*n*=2-3) from three biological replicates.

Data is represented as mean±SD, statistical analysis was performed using one-way ANOVA with Tukey's multiple comparisons or Dunnett's multiple comparisons test. Correlation analysis was performed using Spearman's correlation test (**p*<0.05; ***p*<0.01; ****p*<0.001; *****p*<0.0001).

Pathway specific activation of monocytes induce changes in receptor expression

To investigate how specific signaling pathways dictate TLR4, Siglec-5, and Siglec-9 expression, we used specific inflammatory stimuli to activate and differentiate monocytes. As before, monocytes were purified and subsequently activated with M-CSF to promote macrophage differentiation and survival, and to represent a maturity pathway with a low inflammatory profile [32]. Being key cytokines in OA pathogenesis, IL1β and TNFα were used to replicate an OA microenvironment. LPS was used to specifically activate TLR4 signaling and induce a high inflammatory profile [33,34]. To delineate mechanisms pertaining to the sialylation of the monocytes, sialidase was applied to remove membrane-bound Sia and to assess its effect on cell behavior, specifically regarding the TLR4 pathway.

We assessed the dynamics of TLR4, Siglec-5, and Siglec-9 levels at 0, 4 and 24hrs of stimulation (Figure 2, A-C). An initial increase in TLR4 could be observed already after 4hrs in the media control, M-CSF, and IL1β/TNFα which decreased after 24hrs. In contrast, LPS and sialidase induced a decreased level of TLR4. Siglec-5 decreased across all groups after 4hrs of stimulation but was again upregulated to basal levels by M-CSF and LPS stimulations after 24hrs. All stimulations except sialidase caused an increase in Siglec-9 at 4 and 24hrs compared to basal levels.

M-CSF stimulation for 24hrs increased intermediate monocyte abundance (Figure 2D). LPS stimulation and sialidase activity downregulated the intermediate monocyte population after 4hrs (Supplemental Figure 5A). After 24hrs, the intermediate population was still significantly lower with LPS stimulation, however cells treated with sialidase had recovered this population (Figure 2D).

With the intermediate monocytes expansion induced by M-CSF, expression of TLR4 remained at comparable levels to the media control, a slight decrease in TLR4 was observed with IL1β/TNFα, and a significant decrease was induced by LPS and sialidase (Figure 2E). This inability to upregulate TLR4 by LPS and sialidase was evident already within 4 hours of stimulation (Supplemental Figure 5B). Siglec-5 and Siglec-9 expression was unchanged after 4hrs by all groups except sialidase, which caused a significant downregulation of Siglec-5 (Supplemental Figure, 5C and D). This response to sialidase activity remained after 24hrs, while the other inflammatory stimuli increased the expression of Siglec-5 (Figure 2F). In contrast, no significant alterations in Siglec-9 expression were observed by any stimulations (Figure 2G). The total monocyte population remained Siglec-5^+ and Siglec-9^+ despite fluctuations in expression. The percentage $TLR4^+$ monocytes were highest in the M-CSF and IL1β/TNFα group (Figure 2H).
In summary, TLR4 displayed an interesting dynamic regulation, where it initially increased with M-CSF stimulation but decreased with prolonged LPS stimulation and sialidase activity. Siglec-5 levels initially dropped across all groups but later recovered to basal levels with M-CSF, IL1β/TNFα, and LPS. Sialidase activity uniquely caused sustained Siglec-5 downregulation along with the media control. Siglec-9 increased for all stimulations except after sialidase activity. These results highlight the dynamic and context-dependent regulation of TLR4, Siglec-5, and monocyte subsets that need to be considered in OA-related inflammation. Our data suggests complex regulatory mechanisms govern TLR4 signaling and sialylation, ultimately shaping the monocyte response.

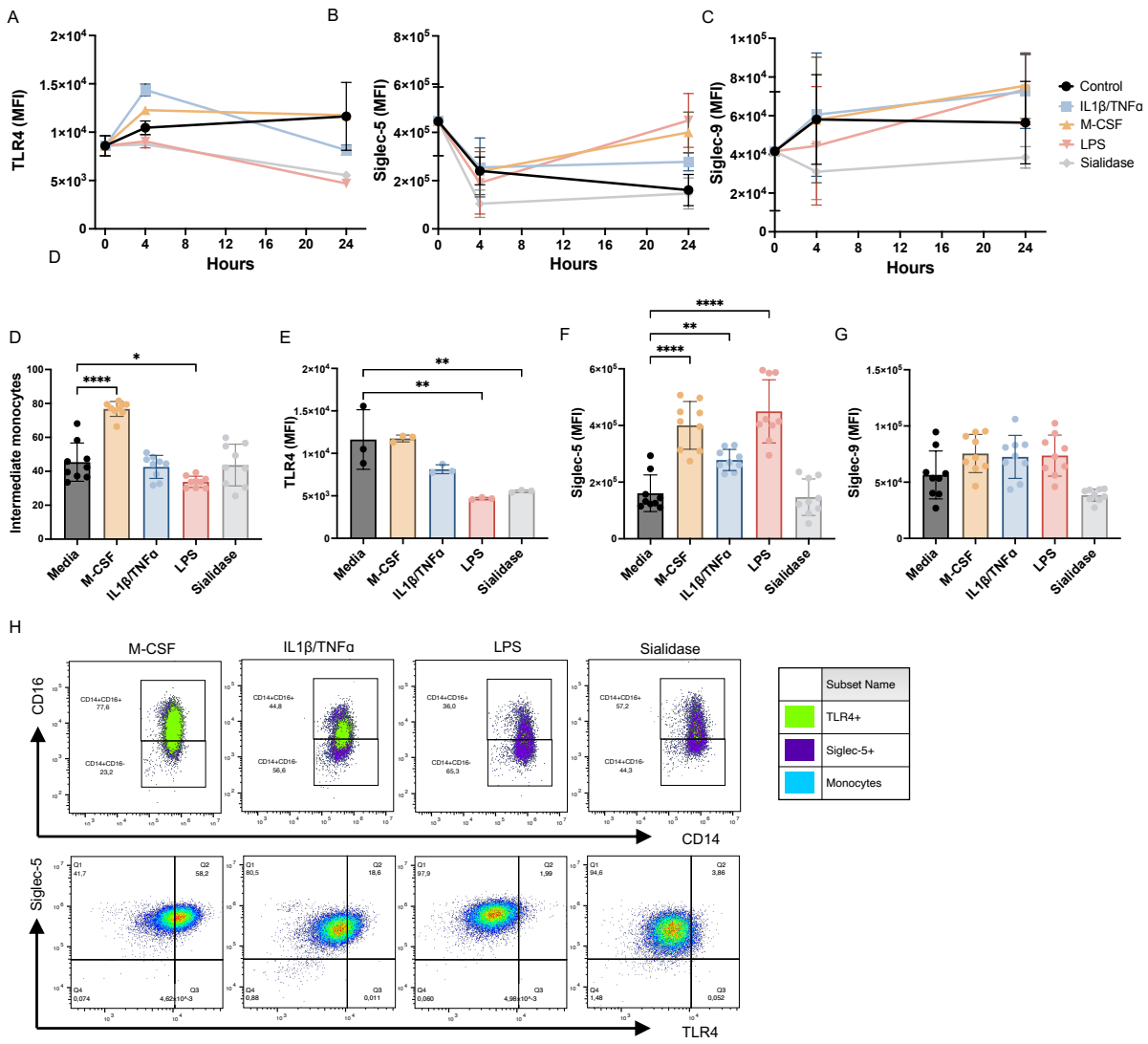

Figure 2. Pathway specific activation of monocytes induce changes in receptor expression

(A-C) MFI of TLR4, Siglec-5, and Siglec-9 at 0, 4, and 24hrs of stimulation with M-CSF, IL1β/TNFα, LPS, and sialidase (*n* = 2-3 from one biological replicate for TLR4, and three biological replicates for Siglec-5 and Siglec-9).

(D) Percentage intermediate monocytes after 24hrs (*n* = 2-3 from three biological replicates).

(E-G) MFI of TLR4, Siglec-5, and Siglec-9 after stimulation for 24hrs (*n* = 2-3 from one biological replicate for TLR4, and three biological replicates for Siglec-5 and Siglec-9).

(H) Representative flow cytometric dot plots displaying the percentage classical and intermediate monocytes where blue represents all cells, purple represents Siglec-5^{+} cells, and green represents TLR4^{+} cells, which can also be displayed in the dot plot below.

Data is represented as mean±SD, statistical analysis was performed using one-way ANOVA with Dunnett's multiple comparisons test (**p*<0.05; ***p*<0.01; ****p*<0.001; *****p*<0.0001).

Monocyte subpopulations exhibit distinct phenotypes and IL-6 production in response to inflammatory stimuli

To further characterize monocyte subpopulations and their functional responses to inflammatory stimuli, we performed clustering analysis based on receptor expression profiles. UMAP clustering (Figure 3A) identified six distinct monocyte populations (Pop1-Pop6), with Pop1 being the largest subset (71,100 cells) and Pop6 being the smallest (238 cells). Heatmap analysis of marker expression (Figure 3B) revealed that CD16 was predominantly expressed in Pop2 and Pop4, while these populations displayed the lowest levels of TLR4. Siglec-5 was upregulated in Pop1, 3, 4, and 6. These data suggest that monocyte subsets differentially regulate receptor expression in response to microenvironment stimuli.

UMAP density contour plots demonstrate the impact of the conditions, including M-CSF, IL1β/TNFα, LPS, sialidase, and SF1-7, on monocyte phenotype distributions (Figure 3C). Notably, M-CSF lead to higher levels of Pop1 and Pop4 compared to IL1β/TNFα, LPS, sialidase. Pop1 and Pop4 are characterized with higher levels of CD16 and Siglec-5, while TLR4 levels are lower compared to most other populations. Comparably, Pop1 and Pop4, along with Pop2 were the most abundant subtypes generated in monocytes stimulated with SF1-7. While monocytes stimulated with SFs display a wide distribution of subpopulations, it was evident that SF5 revealed similarities to the higher inflammatory conditions (IL1β/TNFα, LPS, and sialidase).

To assess the functional consequences of these varying distributions in monocyte phenotypes, IL-6 secretion was measured across each condition (Figure 3D). SF1-7 generated the lowest levels of IL-6 production, ranging from 222-1337 pg/mL, with SF3 and SF5 generating the lowest and highest values, respectively. Inflammatory stimuli significantly increased IL-6 production, with IL1β/TNFα (17,672 pg/mL), LPS (134,034 pg/mL), and sialidase (142,466 pg/mL) inducing the highest levels. M-CSF lead to a moderate (3,142 pg/mL) secretion of IL-6, reflecting its role in promoting macrophage differentiation with a low inflammatory profile.

Overall, these findings highlight that monocyte subpopulations respond differently to inflammatory stimuli, with IL1β/TNFα, LPS, and sialidase driving high IL-6 secretion and distinct receptor expression changes. SF1-7 generate a wide distribution of monocyte populations, with SF5 overlapping more with the high inflammatory-conditions which was also reflected in the IL-6 secretion.

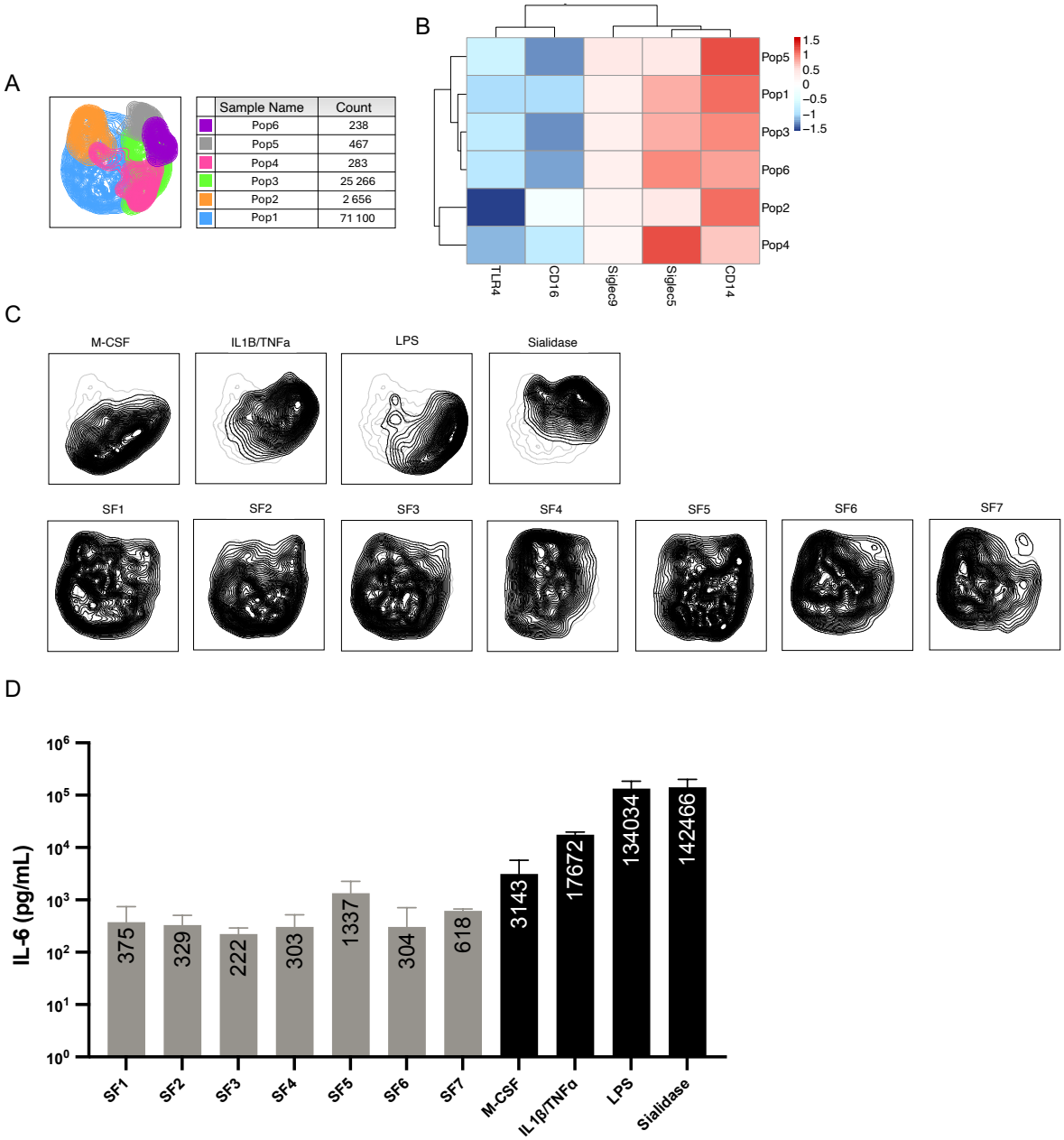

Figure 3. Monocyte subpopulations exhibit distinct phenotypes and IL-6 production in response to inflammatory stimuli

(A) Clustering analysis was performed on concatenated monocytes stimulated with M-CSF, IL1β/TNFα, LPS, sialidase, and SF1-7. Subsequently, monocytes were downsampled to 100,000 cells before performing clustering. This generated six monocyte subpopulations, the table displays each population and its count, respectively.

(B) Heatmap analysis demonstrate the six populations and their relative expression of TLR4, CD16, Siglec-9, Siglec-5, and CD14.

(C) Each UMAP contour density plot represents one condition, i.e. M-CSF, IL1β/TNFα, LPS, sialidase, and SF1-7.

(D) The concentration of IL-6 (pg/mL) produced by the stimulated monocytes were quantified, grey bars represent SFs and black bars represent the pathway-specific stimulations. The mean concentration is observed in each bar (D).

Data is represented as mean±SD. For the monocytes stimulated with SF1-5, three technical replicates were used from three biological replicates. For monocytes stimulated with M-CSF, IL1β/TNFα, LPS, sialidase, three technical replicates were used from one biological replicate.

TAK-242 reduces cytokine secretion and the expression of Siglec-5, while expanding the CD16^{+} monocytes

To further assess the role of TLR4-induced NFkB signaling and its impact on the regulation of CD16, TLR4, Siglec-5, and Siglec-9, we employed the small molecule TLR4 inhibitor TAK-242. This inhibitor specifically binds to Cys747 in the intracellular domain of TLR4, inhibiting both MyD88-independent as well as MyD88-dependent pathways [35]. The involvement of TLR4-signaling was determined by evaluating how effective TAK-242 was in suppressing cytokine production using a multiplex cytokine screening method. The inhibition was performed prior to addition of M-CSF, LPS, and sialidase, and was maintained throughout the experiment.

LPS and sialidase lead to the most pronounced increase in pro-inflammatory cytokine, including TNFα, RANTES, IL-10, and G-CSF, aligning with its known role to trigger TLR4-mediated inflammation (Figure S5A, Figure 4A). M-CSF, in contrast, was associated with lower cytokine secretion consistent with its role in differentiation of monocytes into macrophages. Prominent inhibition of cytokine secretion was observed for both LPS stimulation and sialidase activity, as well as after M-CSF stimulation after both 4 and 24 hours of stimulation. Importantly, we noted that LPS stimulation and sialidase activity resulted in comparable cytokine levels at both timepoints, with a few exceptions observed including IP-10 (CXC10), RANTES, and TNFα. IP-10 was lower in the LPS group compared to sialidase, whereas RANTES was slightly lower in the LPS group at 4hrs and higher in the sialidase group at 24hrs.

Next, we evaluated how blocking TLR4 affected monocyte subsets, particularly the intermediate population, as well as the receptors TLR4, Siglec-5, and Siglec-9. After 4hrs of stimulation, no significant changes in expression of these markers were observed between TAK-242-treated cells or media-treated cells, except for TLR4 expression in the sialidase group (Figure S5B-S5E). However, after 24hrs of activation in presence or absence of TAK-242, we found significant abundance in intermediate monocytes in all groups except IL1β/TNFα (Figure 4B). TAK-242 only induced significant TLR4 expression after M-CSF activation, although a slight increase in the sialidase group was observed (Figure 4C). M-CSF and LPS induced the highest levels of Siglec-5 and interestingly, blocking TLR4 significantly reduced Siglec-5 expression in these two groups (Figure 4D). In contrast, Siglec-9 expression remained unchanged when TLR4 was blocked (Figure 4E). These findings suggest that TAK-242 impacts TLR4 signaling, influencing cytokine production and the regulation of specific monocyte markers, especially Siglec-5 and CD16.

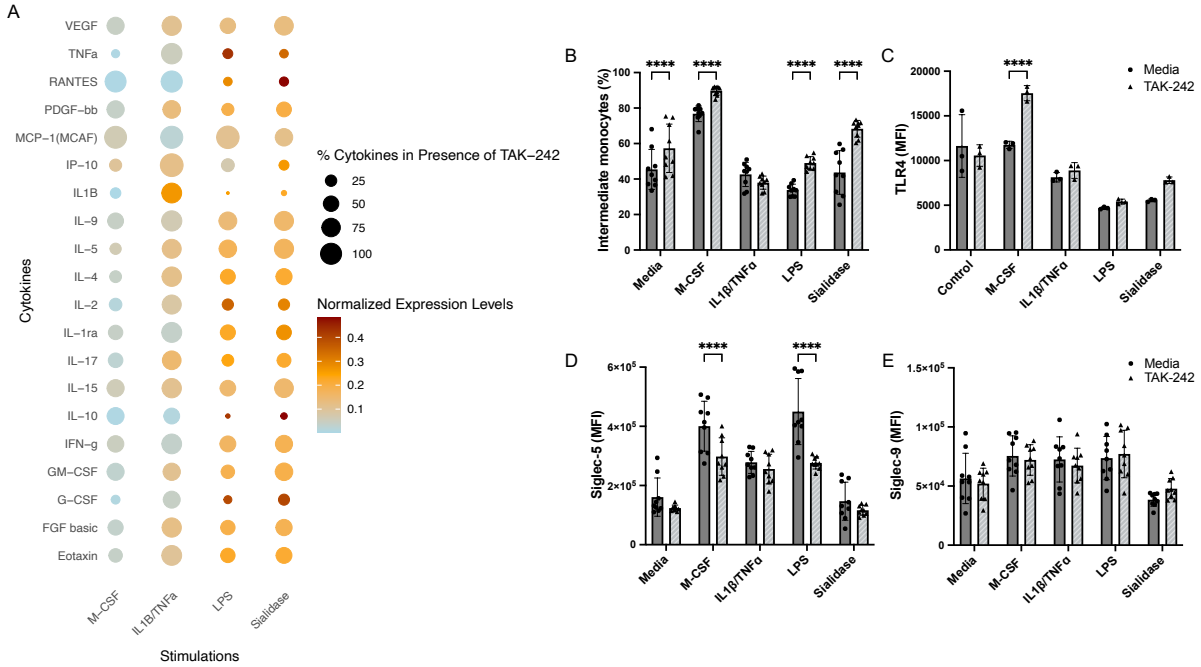

Figure 4. TAK-242 reduces cytokine secretion and the expression of Siglec-5, while expanding the CD16^{+} monocytes

(A) The effect on monocytes imposed by blocking TLR4 with TAK-242 was measured through cytokine production, a panel of cytokines and chemokines were screened after incubation with M-CSF, IL1β/TNFα, LPS, and sialidase for 24hrs with and without TAK-242. Each dataset is the mean of three biological replicates with three technical replicates pooled together.

(B) The percentage of intermediate monocytes was quantified with and without TAK-242 (*n*=2-3 form three biological replicates).

(C-E) MFI of TLR4, Siglec-5, and Siglec-9 was compared between the stimulation in absence or presence of TAK-242 (*n*=2-3 form three biological replicates, except TLR4 which was measured in one biological replicate).

Heatmap analysis display data as fractions where the 0 is the smallest value of each sub column and the largest is the sum of all values in the sub column. Cytokine levels are indicated by Normalized Expression Levels and the % Cytokines in Presence of TAK-242 indicates how effective TAK-242 was at reducing cytokine secretion compared to without TAK-242. Data is represented as mean±SD, statistical analysis was performed using two-way ANOVA with Sidak's multiple comparisons test (*p<0.05; **p<0.01; ***p<0.001; ****p<0.0001).

Siglec-5 and TLR4 colocalization is reduced in cells treated with TAK-242

To investigate the spatial relationship between TLR4 and Siglec-5 in response to M-CSF, LPS and sialidase and the impact of TLR4 inhibition using TAK-242, we performed immunofluorescent staining and quantification of receptor colocalization at 0 and 24hrs. Representative immunofluorescence images show localization of TLR4 (green) and Siglec-5 (yellow) under the different conditions (Figure 5A).

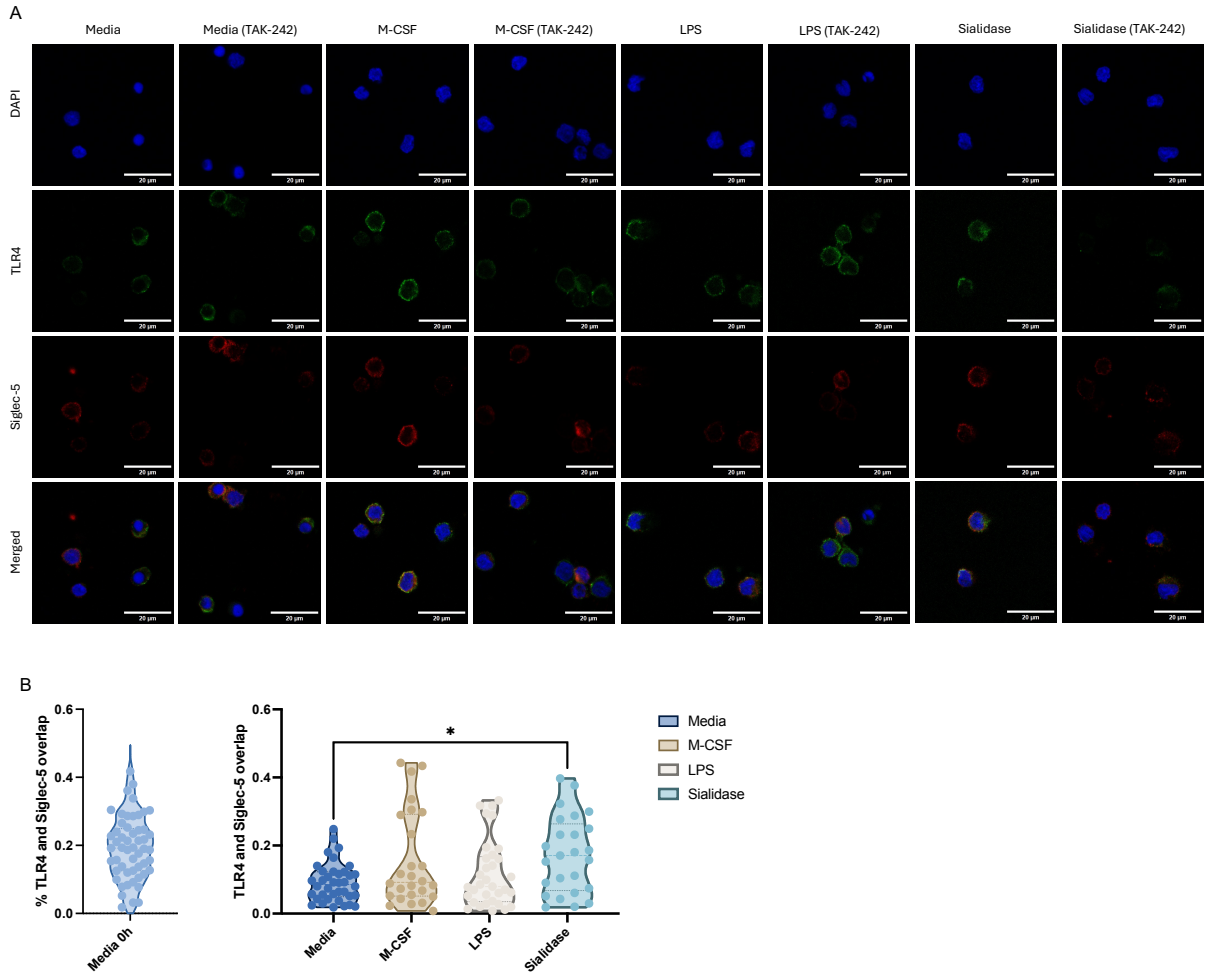

Figure 5. Siglec-5 and TLR4 colocalization is reduced in cells treated with TAK-242

(A) Representative immunofluorescence images of monocytes stimulated with M-CSF, LPS, and sialidase. Scale bar represents 20µm.

(B) Quantification of % colocalization of TLR4 and Siglec-5. Each data point represents one cell, 5-7 images were captured per condition, two biological replicates were used.

Data is represented as mean±SD, statistical analysis was performed using one-way ANOVA with Dunnett's multiple comparisons test (*p<0.05).

DISCUSSION

In this study, we identified Siglec-5 as a key protein in OA pathogenesis using a unique approach involving NPs. By performing proteomics analysis on the protein corona formed around NPs incubated with OA-SF, we detected Siglec-5 as one of 14 most abundant proteins.

The association of Siglec-5 with NPs indicate that this protein could be a relatively rare but functionally significant protein in OA pathogenesis, potentially playing a critical role in immune modulation and inflammation. Through the IntAct Molecular Interaction Database, TLR4 was identified as the protein with the highest confidence score to Siglec-5, indicating strong interaction with potential regulatory mechanisms. While the role of TLR4 has been extensively studied in OA [36], the link to Siglecs remain unclear. We confirmed that essentially all circulating monocytes expressed TLR4, Siglec-5, and Siglec-9. Notably, monocytes stimulated with OA-SF showed increased Siglec-5 expression which inversely correlated with TLR4 expression. Similarly, M-CSF, IL1β/TNFα and LPS generated elevated levels of Siglec-5 compared to the media control. Removal of Sia using sialidase abrogated the cells' ability to upregulate Siglec-5, despite this, LPS and sialidase displayed similar cytokine secretion profiles, indicating high TLR4 activation. Furthermore, TAK-242-mediated TLR4 inhibition reduced Siglec-5 expression, decreased cytokine production, and diminished Siglec-5 and TLR4 colocalization.

We assessed the relative abundance of monocyte subsets after stimulation with OA-SF as well as individual stimulations (M-CSF, IL1β/TNFα, LPS, and sialidase). Already after 4hrs, we observed a lack of non-classical monocytes in all individual stimulation conditions, even the control. This could be due to lack of endothelial interactions necessary for non-classical monocyte survival [37]. Nonetheless, we observed an overall increased abundance of monocytes with an intermediate phenotype ($CD14^+$ $CD16^+$) generated by the different OA-SFs and the individual stimulations (M-CSF, IL1β/TNFα, LPS, and sialidase) after 24hrs. This increase in intermediate monocytes also included differences in abundances generated between the OA-SFs and the individual stimulations which might reflect diversity in SF components depending on the patient. M-CSF generated a large intermediate-like population, likely exhibiting an M2-like phenotype [38]. These findings indicate that SF from OA patients induce monocyte differentiation into intermediate monocytes and that the individual molecular agents used in this study maintain the clinical relevance to aid in delineating specific mechanisms of immune activation.

Siglec-5 had been shown to interact with TLR4, and that murine Siglec-E, facilitate TLR4 internalization [12,23,39]. Similarly, our study found that OA-SF-induced Siglec-5 expression inversely correlates with TLR4 at 24hrs, suggesting potential crosstalk between these receptors. Given that TLR4 is a key driver of proinflammatory activity in OA, its regulation by Siglec-5 may serve as an important immune-modulatory mechanism. Furthermore, we observed that LPS and sialidase significantly reduced TLR4 expression, likely as a desensitization mechanism to prevent monocytes from overreacting to sustained to inflammatory stimuli [40]. It is likely that Siglec-5 might play a role in this desensitization to not exacerbate inflammation. Contradictory to this is the low expression of Siglec-5 in the sialidase group. However, the immunomodulatory effects induced by Siglec-5 might not be strong enough in high-inflammatory conditions such as LPS and sialidase. Depending on the extent to which Siglec-5 exerts its immunomodulatory role, it might act as a key regulator of TLR4 signaling in low-grade inflammation such as in OA, potentially limiting excessive inflammation. Patients with higher Siglec-5 expression may have a more tightly controlled

immune response, preventing the overactivation of TLR4 signaling and associated inflammation.

The role of Siglec-5 in OA and its exact signaling mechanism remains poorly understood. We found that essentially all monocytes stimulated with OA-SF as well as M-CSF, IL1β/TNFα, and LPS exhibited increased Siglec-5 expression compared to the media control at 24hrs. However, compared to monocytes at 0hrs, the overall Siglec-5 expression was lower for most conditions except M-CSF and LPS. A recent study on septic patients demonstrated that soluble Siglec-5 expression modulated $CD8^+$ T-cell proliferation, supporting an immunomodulatory role of Siglec-5 in infection [11]. The same study also revealed that higher levels of soluble Siglec-5 was detected in LPS-stimulated monocytes compared to neutrophils. Monocytes might hence shed Siglec-5 to modulate other immune cells like T cells, which could explain why Siglec-5 was found in high abundance in the NP protein corona as well as why OA-SF stimulated monocytes express less Siglec-5 compared to at 0hrs.

To link distinct monocyte phenotypes with functional mechanisms, we performed clustering analysis and compared the results to IL-6 secretion. UMAP visualization of each stimulatory condition allowed us to map unique features associated with both low- and high-grade inflammation. Our analysis revealed a wide distribution of populations in OA-SF-stimulated monocytes, with a more uniform distribution in monocytes stimulated with M-CSF, IL1β/TNFα, LPS, and sialidase. Specifically, OA-SF-stimulation resulted in a high abundance of monocytes with low TLR4 and high CD16, while Siglec-5 varied (Pop1, Pop2, Pop4). This heterogeneity suggests OA-SF activated monocytes through multiple pathways. In contrast, high-grade inflammatory conditions displayed a monocytes phenotype characterized by with CD16, medium TLR4, but also variable Siglec-5 expression (Pop3, Pop5, Pop6). Interestingly, SF5 exhibited a profile similar to high-grade inflammatory conditions, correlating with increased IL-6 secretion compared to other SFs. Notably, OA-SF-stimulated monocytes shared the most similarities with M-CSF-stimulated monocytes, which could explain the observed low-grade inflammatory response. These finding highlight how interpatient variability influence subtle changes in monocyte surface markers, ultimately shaping inflammatory responses.

Notably, monocytes stimulated with LPS and sialidase exhibited highly similar cytokine secretion profiles, reflecting their shared activation through TLR4 signaling. This was further validated using the TLR4 inhibitor TAK-242, which significantly reduced cytokine secretion in both conditions. However, TAK-242 appeared to be more effective in LPS-stimulated monocytes, as cytokines levels - including VEGF, PDGF, IL-17, IL-15, IL-10, GM-CSF, G-CSF, FGF basic, and Eotaxin – were slightly lower in LPS-stimulated cells compared to sialidase treated cells after 24hrs. Although, sialidase-induced activation predominantly occurs through TLR4, the discrepancy between LPS and sialidase responses suggests that sialidase may influence additional signaling pathways or that the loss of Sia may impair cellular recovery mechanism.

Both Siglec and TLR4 expression can be influenced by complex interactions with glycan structures, particularly α2,3 and α2,6 Sia linkages. These glycan modifications can modulate immune cell signaling and are often altered in response to inflammation [41,42]. Low levels of Siglec-5 in the sialidase group indicate that its expression is governed by the presence of Sia, either on the host cell or on neighboring cells. Several studies [43,44] have demonstrated changes in surface sialylation in OA chondrocytes and fibroblast-like synoviocytes in rheumatoid arthritis, indicating that inflammation significantly affects glycosylation patterns. The elevated Siglec-5 expression in OA-SF-stimulated monocytes compared to the media control may reflect an adaptive response linked to glycan remodeling processes, potentially indicating shifts in sialylation patterns that impact monocyte function and the broader inflammatory environment in OA.

We acknowledge some key limitations to our study. While this study has focused on monocytes, many different cells are involved in OA, including chondrocytes and synoviocytes. The transient increases in Siglec-5, alongside persistent decreases in α2,3 and α2,6 Sia, suggest ongoing glycan remodeling that may involve TLR4 or other receptors. Longer observation periods and dose-dependent studies, particularly with sialidase, are needed to clarify these dynamics. Broader investigation into glycosylation patterns and their impact on immune receptor networks could uncover additional therapeutic targets. Future work should also validate these findings in vivo and in human OA samples, focusing on how sialylation patterns and Siglec-5 expression vary among patient subgroups.
In conclusion, this study highlights the role of TLR4 and Siglec-5 in the pathogenesis of OA, shedding light on their intricate interplay. While both receptors are implicated in the inflammatory process of OA, their complex relationship warrants further investigation to fully elucidate the underlying mechanisms. The marked reduction in cytokine production upon TLR4 inhibition underscores the therapeutic potential of TAK-242 particularly for patient subgroups with low Siglec-5 expression, where modulation of TLR4 signaling may prove especially beneficial. Similar features imposed on monocytes by LPS and sialidase demonstrated TLR4-specific activation. Yet, sialidase failed to upregulate Siglec-5, emphasizing an important role of α2,6 Sia as ligand which could serve as a potential therapeutic target for immune cell modulation. Given that Siglec-5 shares key signaling domains with PD-1, restoring Siglec-5 function and understanding its signaling mechanisms presents promising opportunities to modulate TLR4 signaling and reduce inflammation not only in OA, but for many pathogeneses where Siglec-5 is involved.

MATERIALS AND METHODS

Sex as a biological variable

This study includes patient material from both female and male patients. Synovial fluid from 7 OA patients (2 females) due for total knee replacement surgery was selected for the experiments: age 63-87 (Median 77) and BMI 23.4-38.0 (Median 25.6). Due to the small patient population, no further stratification was made.

Protein corona isolation and Material synthesis

NP synthesis was previously described in von Mentzer *et al*[6]. Briefly, PAMAM (G5) were modified by PEGylation using PEG 350 MW, NP_{350} at 2%, or PEG 5000 MW, NP_{5000} at 2%, purified, and used at a the final concentration of 30 µM in PBS (pH = 7.4).

SF samples from 5 4 (2f/2m, 45–82 years old) late OA patients were collected during aseptic aspiration of knee joints at the Rheumatology Clinic and Orthopaedic Clinic, respectively, at Sahlgrenska University Hospital, Gothenburg, Sweden.
Patient SF were pooled, diluted 1:20 in PBS, and mixed with 30 µM NP solution (1:1, v/v). The samples were incubated at 37°C while shaking for 1 h at 100 rpm to resemble the dynamic environment of the SF in the joint and address the Vroman effect. To preserve the proteins bound with high affinity known as the hard protein coronas, NPs were spun down at 15,000 × *g* for 15 min and washed three times with chilled PBS. Final concentration of NP-protein complexes was 1 µg/mL (2.5×10^8 particles/mL).

NPs were pelleted by centrifugation at 15,000 × *g* for 15 min, snap-frozen using liquid nitrogen, and submitted to the Proteomics Core Facility (Gothenburg, Sweden). Briefly, proteins were digested into peptides using MS-grade trypsin and analyzed by nanoscale liquid chromatography-tandem mass spectrometry LC-MS/MS. The mascot search engine was used to match the discovered peptide sequences against SwissProt human and bovine protein database using Proteome Discoverer. Data were analyzed using a label-free quantification method and the protein false discovery rate was set to 1%. To elucidate the molecular functions and classifications of significant proteins, the enrichment analysis was performed using Gene Ontology-based PANTHER classification system. SF samples were matched to human (*Homo sapiens*), while FCS samples were matched to the bovine (*Bos taurus*) databases.

Monocyte isolation

Buffy coats obtained from the blood bank at Sahlgrenska University Hospital, Gothenburg, Sweden (18/23) were prepared the day before and collected for the experimental study in the morning. Monocyte isolation was performed using the negative selection RosettSep™ Human Monocyte Enrichment Cocktail (Stemcell Technologies). Since this kit is optimized for whole blood, the buffy coat was diluted 1:1 with Dulbecco's phosphate buffered saline (PBS) (Gibco) to ensure that the concentration of nucleated cells did not exceed the limit. Apart from that, the isolation was performed according to the protocol. Briefly, the blood was mixed

with the cocktail and incubated for 20 min at room temperature. Following this, the mixture was placed over a Ficoll-Paque (Cytiva) density gradient medium and centrifuged in a swing-out bucket for 20 min at 1200 x g with the brake off. The enriched monocytes were transferred to a new tube and washed in the recommended medium containing PBS, 2% heat inactivated fetal bovine serum (FBS, Gibco, Paisley, UK), and 1mM EDTA (Thermo-fisher). After this, the monocytes were washed twice in recommended medium and centrifuged at 300 x g for 10 min with the brake low.

Monocyte stimulations

The enriched monocytes were counted and plated at a concentration of 3 x 10^5 cells/well in a 48 well plate (Costar). The cells were diluted in RPMI Medium 1640 (Gibco, Paisley, UK) supplemented with 1 % glutaMAX (Gibco, Grand Island, USA), 1 % Penicillin/Streptomycin and 10 % FBS. TAK-242 (Merck) was added to the designated wells at a concentration of 1µM and incubated for one hour. The final concentration of each stimulation was 10ng/mL of IL1β and TNFα, 100ng/mL M-CSF, 100ng/mL LPS, and 100mU/mL sialidase (Sigma-Aldrich, N2876). The cells were analyzed after 0, 4, and 24 hours.
As a comparison to these commonly used stimulations, we incubated primary monocytes with OA synovial fluid at a concentration of 25%. After 24hrs of stimulation the surface markers were detected using flow cytometry.

Flow cytometric analysis

Monocytes were collected by transferring the whole volume to a v-plate (Costar) and centrifuging them at 300 x g for 5 minutes, 4°C. The supernatants were transferred and saved at -80°C for cytokine measurement. Meanwhile, to detach the monocytes that started differentiating into macrophages, 50µL trypsin-EDTA (Gibco) was added. Once detached, 50µL ice cold recommended medium was used to inactivate trypsin. The detached cells were added to the v-plate and washed twice. 10µL Fc block (Biolegend) was added to each well and the plate was incubated on ice for 10 min. Monocyte phenotypes were analyzed using the following antibodies at a final concentration of 1:100, CD14-FITC, CD16-Brilliant Violet 605, Siglec-5-PE, Siglect-9-PE-Cy7, and TLR4-APC (Biolegend). 10µL the antibody cocktail was added to each well and the plate was incubated for 20 min on ice in the dark. The cells were washed three times in recommended medium. To exclude dead cells, 1µM DAPI (Biolegend) was added. Fluorescence minus one (FMO) and unstained cells were used to set up the gating. The cells were run on the Cytoflex LX (Beckman Coulter) and analyzed using FlowJo (Version 10.10.0).

Bio-Plex Pro Human Cytokine Grp I Panel 27-Plex

Supernatants from the monocyte stimulation assays were screened for a panel of 27 cytokines and chemokines to evaluate the immune response in the different conditions. The technical replicates from three biological replicates were combined, respectively, to reduce the number of wells to one well per biological replicate. The assay was performed according to the manufacturer's instructions. Briefly, vortexed beads were added to each well, followed by two washing steps. Samples were centrifuged at 1,000 x g for 15 min at 4°C prior being added to the plate along with the standard, blank, and control. The plate was incubated shaking at 850

rpm for 30 min, followed by three washing steps. Detection antibodies were added to each well and incubated shaking for 30 min. After three washings, streptavidin-PE was added and incubated shaking for 10 min. An additional three washings were performed before resuspending the beads in assay buffer and reading the plate.
For values that were out of range, extrapolated values were assumed based on the highest and lowest value of the standard curve. We observed that most of the groups was below detection level for IL-7 and above detection level for MIP-1α, MIP-1β, IL-6, and IL-8 and they were hence removed. Additionally, the media control was below detection level for most analytes and thus removed.

Confocal microscopy
To analyze TLR4 and Siglec-5 colocalization, confocal imaging was performed. $1.2x10^6$ isolated monocytes were seeded in complete RPMI in 12 well plates and pre-treated with 1µM TAK-242 or PBS, for 1 hour. Following this, the stimulations M-CSF, LPS, and Sialidase were added accorded to previously mentioned concentrations. After 0 and 24h, the monocytes were transferred to Eppendorf tubes and the leftover attached cells were trypsinized and transferred to the tubes before being centrifuged at 1,500 rpm for 5 min. The supernatant was discarded, and the cells were washed with PBS and centrifuged to remove the supernatant, this was performed three times. To fix the cells, 100µL 4% paraformaldehyde (PFA) was added to each tube and incubated at room temperature for 10 min. Detection was performed using anti-human TLR4 mouse monoclonal antibody (HTA-125, Invitrogen) and anti-human Siglec-5 rabbit polyclonal antibody (13230-1-AP, Proteintech), both diluted 1:100 and stained for 1h in room temperature. 2 µg/mL of secondary antibody goat anti-mouse IgG (A32723, Thermo Fisher) and goat anti-rabbit IgG (A21245, Thermo Fisher) was incubated in the dark for 1h. After washing, the cells were spun onto a glass slide, ProLong™ Gold Antifade Mountant (Invitrogen) was added before mounting the cover slip. Images were acquired by using an inverted Nikon C2+ confocal microscope (Nikon Instruments, Amsterdam, Netherlands) equipped with a C2-DUVB GaAsP detector unit offering variable emission bandpass settings. A 60x Nikon APO oil-immersion objective (numerical aperture 1.4). Excitation and emission were set as follows for different staining: DAPI - λ_{ex} 401 nm, λ_{em} 425-497 nm, goat anti-rabbit IgG (Alexa Fluor 647) - λ_{ex} 639 nm, λ_{em} 644-695 nm, and goat anti-mouse IgG (Alexa Fluor 488) - λ_{ex} 489 nm, λ_{em} 503-546 nm.

Image analysis
The confocal images displayed in figure 4B were enhanced for illustrative purposes. The intensity was increased the same across all images. MFI extracted of the confocal images was performed on the original intensity profiles with no alterations.

Statistics
Statistical significance was performed using Prism (GraphPad software). Data are shown as the mean and standard deviation and statistical differences were analyzed using One-way followed by Tukey's or Dunnett's multiple comparisons test or two-way ANOVA followed by Sidak's multiple comparisons test. Correlation was analyzed using Spearman correlation analysis. All statistical details can be obtained in the figure legends.

Study approval
The studies involving human participants were reviewed and approved by the Regional Ethical Review Board in Gothenburg. All patients provided informed consent and the procedure was approved by the Ethics Committee of Gothenburg University (Ethical approval Dnr: 573-07, 172-15).

Data availability
The original contributions presented in the study are included in the article or Supplemental Material; further inquiries can be directed to the corresponding author.

Author Contributions
Study design (L.R, A.S), conducting experiments (L.R, F.J), acquiring data (L.R, F.J), analyzing data (L.R, F.J, N.K, A.S), providing funding and reagents (N.K, A,S), writing the manuscript (L.R, A.S). All authors have contributed to editing and approved the manuscript.

Acknowledgements:
Anna-Karin Hultgård-Ekwall, Lena Björkman, Thomas Eisler, and Ola Rolfson are gratefully acknowledged for arranging the patient samples, and Sofia Grindberg and Paula-Therese Kelly Pettersson at Danderyd's Hospital and Lotta Falkendahl at the University of Gothenburg are acknowledged for their assistance in collecting the samples. This work was supported by Chalmers Technical University and its Area of Advance Nano. The authors greatly acknowledge further financial support from the Foundation for Sigurd and Elsa Goljes Minne (LA2021-0100), The Royal Swedish Academy of Sciences (CR2021-0024), The Jeanssons Foundation (J2021-0050), The Hasselblad Foundation, the Swedish Research Council (2021-01870), Wilhelm och Martina Lundgrens Vetenskapsfond (2022-4054) the Swedish Rheumatism Association (R-981253), the King Gustav V's 80 years' foundation (FAI-2022-0872) and IngaBritt och Arne Lundbergs Forskningsstiftelse (LU2022-0041).

References

1. Courties, A., Kouki, I., Soliman, N., Mathieu, S., and Sellam, J. (2024). Osteoarthritis year in review 2024: Epidemiology and therapy. Osteoarthritis Cartilage *32*, 1397-1404. 10.1016/j.joca.2024.07.014.
2. Ye, Z., Wang, Y., Xiang, B., Wang, H., Tao, H., Zhang, C., Zhang, S., Sun, D., Luo, F., and Song, L. (2023). Roles of the Siglec family in bone and bone homeostasis. Biomed Pharmacother *165*, 115064. 10.1016/j.biopha.2023.115064.
3. Zhang, H., Cai, D., and Bai, X. (2020). Macrophages regulate the progression of osteoarthritis. Osteoarthritis and Cartilage *28*, 555-561. 10.1016/j.joca.2020.01.007.
4. Zhu, X., Lee, C.-W., Xu, H., Wang, Y.-F., Yung, P.S.H., Jiang, Y., and Lee, O.K. (2021). Phenotypic alteration of macrophages during osteoarthritis: a systematic review. Arthritis Research & Therapy *23*. 10.1186/s13075-021-02457-3.
5. Yin, X., Wang, Q., Tang, Y., Wang, T., Zhang, Y., and Yu, T. (2024). Research progress on macrophage polarization during osteoarthritis disease progression: a review. Journal of Orthopaedic Surgery and Research *19*. 10.1186/s13018-024-05052-9.
6. von Mentzer, U., Sellden, T., Raberg, L., Erensoy, G., Hultgard Ekwall, A.K., and Stubelius, A. (2022). Synovial fluid profile dictates nanoparticle uptake into cartilage - implications of the protein corona for novel arthritis treatments. Osteoarthritis Cartilage *30*, 1356-1364. 10.1016/j.joca.2022.07.002.
7. Vuchkovska, A., Glanville, D.G., Scurti, G.M., Nishimura, M.I., White, P., Ulijasz, A.T., and Iwashima, M. (2022). Siglec-5 is an inhibitory immune checkpoint molecule for human T cells. Immunology *166*, 238-248. 10.1111/imm.13470.
8. Matsumoto, T., Takahashi, N., Kojima, T., Yoshioka, Y., Ishikawa, J., Furukawa, K., Ono, K., Sawada, M., Ishiguro, N., and Yamamoto, A. (2016). Soluble Siglec-9 suppresses arthritis in a collagen-induced arthritis mouse model and inhibits M1 activation of RAW264.7 macrophages. Arthritis Res Ther *18*, 133. 10.1186/s13075-016-1035-9.
9. Wang, X., Liu, D., Ning, Y., Liu, J., Wang, X., Tu, R., Shen, H., Chen, Q., and Xiong, Y. (2017). Siglec-9 is upregulated in rheumatoid arthritis and suppresses collagen-induced arthritis through reciprocal regulation of Th17-/Treg-cell differentiation. Scand J Immunol *85*, 433-440. 10.1111/sji.12543.
10. Dou, C., Zhen, G., Dan, Y., Wan, M., Limjunyawong, N., and Cao, X. (2022). Sialylation of TLR2 initiates osteoclast fusion. Bone Research *10*, 24. 10.1038/s41413-022-00186-0.
11. Lozano-Rodríguez, R., Avendaño-Ortíz, J., Montalbán-Hernández, K., Ruiz-Rodríguez, J.C., Ferrer, R., Martín-Quirós, A., Maroun-Eid, C., González-López, J.J., Fàbrega, A., Terrón-Arcos, V., et al. (2023). The prognostic impact of SIGLEC5-induced impairment of CD8+ T cell activation in sepsis. eBioMedicine *97*, 104841. 10.1016/j.ebiom.2023.104841.
12. Chen, G.Y., Brown, N.K., Wu, W., Khedri, Z., Yu, H., Chen, X., van de Vlekkert, D., D'Azzo, A., Zheng, P., and Liu, Y. (2014). Broad and direct interaction between TLR and Siglec families of pattern recognition receptors and its regulation by Neu1. Elife *3*, e04066. 10.7554/eLife.04066.
13. Kukan, E.N., Fabiano, G.L., and Cobb, B.A. (2024). Siglecs as modulators of macrophage phenotype and function. Semin Immunol *73*, 101887. 10.1016/j.smim.2024.101887.
14. Chou, C.-H., Jain, V., Gibson, J., Attarian, D.E., Haraden, C.A., Yohn, C.B., Laberge, R.-M., Gregory, S., and Kraus, V.B. (2020). Synovial cell cross-talk with cartilage plays a major role in the pathogenesis of osteoarthritis. Scientific Reports *10*. 10.1038/s41598-020-67730-y.

15. Gómez-Aristizábal, A., Gandhi, R., Mahomed, N.N., Marshall, K.W., and Viswanathan, S. (2019). Synovial fluid monocyte/macrophage subsets and their correlation to patient-reported outcomes in osteoarthritic patients: a cohort study. Arthritis Research & Therapy *21*. 10.1186/s13075-018-1798-2.
16. Rapp, A.E., and Zaucke, F. (2023). Cartilage extracellular matrix-derived matrikines in osteoarthritis. Am J Physiol Cell Physiol *324*, C377-C394. 10.1152/ajpcell.00464.2022.
17. von Mentzer, U., Corciulo, C., and Stubelius, A. (2022). Biomaterial Integration in the Joint: Pathological Considerations, Immunomodulation, and the Extracellular Matrix. Macromol Biosci *22*, e2200037. 10.1002/mabi.202200037.
18. Huang, S., Thomsson, K.A., Jin, C., Ryberg, H., Das, N., Struglics, A., Rolfson, O., Björkman, L.I., Eisler, T., Schmidt, T.A., et al. (2022). Truncated lubricin glycans in osteoarthritis stimulate the synoviocyte secretion of VEGFA, IL-8, and MIP-1α: Interplay between O-linked glycosylation and inflammatory cytokines. Frontiers in Molecular Biosciences *9*. 10.3389/fmolb.2022.942406.
19. Barreto, G., Senturk, B., Colombo, L., Brück, O., Neidenbach, P., Salzmann, G., Zenobi-Wong, M., and Rottmar, M. (2020). Lumican is upregulated in osteoarthritis and contributes to TLR4-induced pro-inflammatory activation of cartilage degradation and macrophage polarization. Osteoarthritis and Cartilage *28*, 92-101. 10.1016/j.joca.2019.10.011.
20. Barreto, G., Manninen, M., and K. Eklund, K. (2020). Osteoarthritis and Toll-Like Receptors: When Innate Immunity Meets Chondrocyte Apoptosis. Biology *9*, 65. 10.3390/biology9040065.
21. Tsuno, H., Tanaka, N., Naito, M., Ohashi, S., Iwasawa, M., Kadoguchi, T., Mitomi, H., Matsui, T., Furukawa, H., and Fukui, N. (2023). Analysis of proteins released from osteoarthritic cartilage by compressive loading. Scientific Reports *13*. 10.1038/s41598-023-45472-x.
22. Warmink, K., Vinod, P., Korthagen, N.M., Weinans, H., and Rios, J.L. (2023). Macrophage-Driven Inflammation in Metabolic Osteoarthritis: Implications for Biomarker and Therapy Development. International Journal of Molecular Sciences *24*, 6112. 10.3390/ijms24076112.
23. Wu, Y., Ren, D., and Chen, G.-Y. (2016). Siglec-E Negatively Regulates the Activation of TLR4 by Controlling Its Endocytosis. The Journal of Immunology *197*, 3336-3347. 10.4049/jimmunol.1600772.
24. Feng, C., Stamatos, N.M., Dragan, A.I., Medvedev, A., Whitford, M., Zhang, L., Song, C., Rallabhandi, P., Cole, L., Nhu, Q.M., et al. (2012). Sialyl residues modulate LPS-mediated signaling through the Toll-like receptor 4 complex. PLoS One *7*, e32359. 10.1371/journal.pone.0032359.
25. Allendorf, D.H., Franssen, E.H., and Brown, G.C. (2020). Lipopolysaccharide activates microglia via neuraminidase 1 desialylation of Toll-like Receptor 4. Journal of Neurochemistry *155*, 403-416. 10.1111/jnc.15024.
26. Liang, F., Seyrantepe, V., Landry, K., Ahmad, R., Ahmad, A., Stamatos, N.M., and Pshezhetsky, A.V. (2006). Monocyte Differentiation Up-regulates the Expression of the Lysosomal Sialidase, Neu1, and Triggers Its Targeting to the Plasma Membrane via Major Histocompatibility Complex Class II-positive Compartments. Journal of Biological Chemistry *281*, 27526-27538. 10.1074/jbc.m605633200.
27. Silva, Z., Rabaca, J.A., Luz, V., Lourenco, R.A., Salio, M., Oliveira, A.C., Bule, P., Springer, S., and Videira, P.A. (2024). New insights into the immunomodulatory potential of sialic acid on monocyte-derived dendritic cells. Cancer Immunol Immunother *74*, 9. 10.1007/s00262-024-03863-7.

28. Bull, C., Collado-Camps, E., Kers-Rebel, E.D., Heise, T., Sondergaard, J.N., den Brok, M.H., Schulte, B.M., Boltje, T.J., and Adema, G.J. (2017). Metabolic sialic acid blockade lowers the activation threshold of moDCs for TLR stimulation. Immunol Cell Biol *95*, 408-415. 10.1038/icb.2016.105.
29. Kapellos, T.S., Bonaguro, L., Gemünd, I., Reusch, N., Saglam, A., Hinkley, E.R., and Schultze, J.L. (2019). Human Monocyte Subsets and Phenotypes in Major Chronic Inflammatory Diseases. Frontiers in Immunology *10*. 10.3389/fimmu.2019.02035.
30. Williams, H., Mack, C., Baraz, R., Marimuthu, R., Naralashetty, S., Li, S., and Medbury, H. (2023). Monocyte Differentiation and Heterogeneity: Inter-Subset and Interindividual Differences. International Journal of Molecular Sciences *24*, 8757. 10.3390/ijms24108757.
31. Snodgrass, R.G., Jiang, X., and Stephensen, C.B. (2022). Monocyte subsets display age-dependent alterations at fasting and undergo non-age-dependent changes following consumption of a meal. Immunity & Ageing *19*. 10.1186/s12979-022-00297-6.
32. Harber, K.J., Nguyen, T.A., Schomakers, B.V., Heister, D.A.F., de Vries, H.E., van Weeghel, M., Van den Bossche, J., and de Winther, M.P.J. (2024). Adenine is an anti-inflammatory metabolite found to be more abundant in M-CSF over GM-CSF-differentiated human macrophages. Immunol Lett *265*, 23-30. 10.1016/j.imlet.2023.12.003.
33. Zamyatina, A., and Heine, H. (2020). Lipopolysaccharide Recognition in the Crossroads of TLR4 and Caspase-4/11 Mediated Inflammatory Pathways. Frontiers in Immunology *11*. 10.3389/fimmu.2020.585146.
34. Park, B.S., and Lee, J.-O. (2013). Recognition of lipopolysaccharide pattern by TLR4 complexes. Experimental & Molecular Medicine *45*, e66-e66. 10.1038/emm.2013.97.
35. Takashima, K., Matsunaga, N., Yoshimatsu, M., Hazeki, K., Kaisho, T., Uekata, M., Hazeki, O., Akira, S., Iizawa, Y., and Ii, M. (2009). Analysis of binding site for the novel small-molecule TLR4 signal transduction inhibitor TAK-242 and its therapeutic effect on mouse sepsis model. Br J Pharmacol *157*, 1250-1262. 10.1111/j.1476-5381.2009.00297.x.
36. Bartels, Y.L., Van Lent, P.L.E.M., Van Der Kraan, P.M., Blom, A.B., Bonger, K.M., and Van Den Bosch, M.H.J. (2024). Inhibition of TLR4 signalling to dampen joint inflammation in osteoarthritis. Rheumatology *63*, 608-618. 10.1093/rheumatology/kead493.
37. Mildner, A., Kim, K.-W., and Yona, S. (2024). Unravelling monocyte functions: from the guardians of health to the regulators of disease. Discovery Immunology *3*. 10.1093/discim/kyae014.
38. Chen, Y.-C., Lai, Y.-S., Hsuuw, Y.-D., and Chang, K.-T. (2021). Withholding of M-CSF Supplement Reprograms Macrophages to M2-Like via Endogenous CSF-1 Activation. International Journal of Molecular Sciences *22*, 3532. 10.3390/ijms22073532.
39. Boyd, C.R., Orr, S.J., Spence, S., Burrows, J.F., Elliott, J., Carroll, H.P., Brennan, K., Gabhann, J.N., Coulter, W.A., Johnston, J.A., and Jefferies, C.A. (2009). Siglec-E Is Up-Regulated and Phosphorylated Following Lipopolysaccharide Stimulation in Order to Limit TLR-Driven Cytokine Production. The Journal of Immunology *183*, 7703-7709. 10.4049/jimmunol.0902780.
40. Ciesielska, A., Matyjek, M., and Kwiatkowska, K. (2021). TLR4 and CD14 trafficking and its influence on LPS-induced pro-inflammatory signaling. Cellular and Molecular Life Sciences *78*, 1233-1261. 10.1007/s00018-020-03656-y.
41. Miyagi, T., and Yamaguchi, K. (2012). Mammalian sialidases: Physiological and pathological roles in cellular functions. Glycobiology *22*, 880-896. 10.1093/glycob/cws057.
42. Aljohani, M.A., Sasaki, H., and Sun, X.L. (2024). Cellular translocation and secretion of sialidases. J Biol Chem *300*, 107671. 10.1016/j.jbc.2024.107671.

43. Carpintero-Fernandez, P., Varela-Eirin, M., Lacetera, A., Gago-Fuentes, R., Fonseca, E., Martin-Santamaria, S., and Mayan, M.D. (2020). New Therapeutic Strategies for Osteoarthritis by Targeting Sialic Acid Receptors. Biomolecules *10*, 637. 10.3390/biom10040637.
44. Wang, Y., Khan, A., Antonopoulos, A., Bouché, L., Buckley, C.D., Filer, A., Raza, K., Li, K.-P., Tolusso, B., Gremese, E., et al. (2021). Loss of α2-6 sialylation promotes the transformation of synovial fibroblasts into a pro-inflammatory phenotype in arthritis. Nature Communications *12*. 10.1038/s41467-021-22365-z.